

Fabrication and Study of Parameters and Properties of Nanostructured Membranes for MEMS Devices

N. A. Dyuzhev^{a,*}, E. E. Gusev^a, T. A. Gryazneva^a, A. A. Dedkova^a, D. A. Dronova^a,
V. Yu. Kireev^a, E. P. Kirilenko^a, D. M. Migunov^a, D. V. Novikov^a, N. N. Patyukov^a,
A. A. Presnukhina^a, A. D. Bakun^b, and D. S. Ermakov^b

^aNational Research University “Moscow Institute of Electronic Technology”, Zelenograd, Moscow, 123398 Russia

^bNational Research Nuclear University “Moscow Engineering Physics Institute”, Moscow, 115409 Russia

*e-mail: bubbledouble@mail.ru

Received November 17, 2016; in final form, June 21, 2017

Abstract—The technology of forming blanks of nanostructured membranes for MEMS devices based on alternating $\text{Si}_3\text{N}_4/\text{SiO}_2$ layers with a nanometer thickness has been developed. A comprehensive study of the structure and composition of membranes using microanalysis methods based on spectroscopic ellipsometry, scanning electron microscopy (SEM), secondary ion mass spectrometry (SIMS), Auger electron spectroscopy (AES), probe profilometry, and X-ray diffractometry is performed. The mechanical stress in silicon wafers with blanks of nanostructured membranes is experimentally determined.

DOI: 10.1134/S1995078017040073

INTRODUCTION

In many devices based on MEMS elements, such as gas flow, pressure, electromagnetic radiation, object velocity, and acceleration sensors, a number of basic working parameters are determined by the characteristics of membranes on which the sensitive elements (sensors) of these devices are formed. Indeed, the mechanical, thermal, optical, and dielectric properties of membranes to a large extent determine the sensitivity of the sensor to the measured impacts [1, 2].

Figure 1 shows a gas-flow sensor based on two thin-film platinum thermoresistors and the thin-film platinum heating element formed on a dielectric membrane consisting of four alternating layers of silicon oxide and nitride $\text{SiO}_2(0.6 \mu\text{m})/\text{Si}_3\text{N}_4(0.13 \mu\text{m})/\text{SiO}_2(0.3 \mu\text{m})/\text{Si}_3\text{N}_4(0.13 \mu\text{m})$. The sensitivity of such a sensor to the measured gas flow depends on the specific resistance and temperature resistance coefficient (TRC) of platinum thermoresistors, as well as the heat conduction and heat capacity of the dielectric membrane [3].

For reducing the heat conduction and heat capacity of dielectric membranes in order to increase the sensor sensitivity, the membrane thickness should be as minimal as possible. The lower limit of the dielectric membrane thickness is determined by its mechanical strength and depends on the material of applied layers and methods and modes of their formation.

The ratio of SiO_2 and Si_3N_4 layer thickness in blanks of the applied microstructured membranes

(membranes with layers whose thickness is in a range of 0.1–1.0 μm) is chosen from the condition of obtaining small tensile stress in wafers with silicon oxide and nitride layers. Under this condition, silicon through etching and membrane formation should

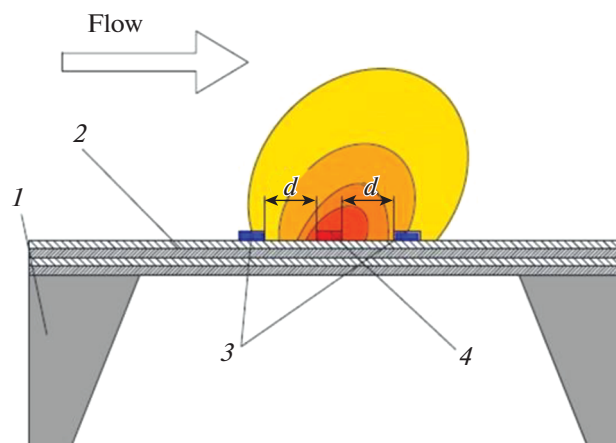


Fig. 1. (Color online) Schematic diagram of the gas-flow sensor manufactured with the membrane formed on the silicon wafer: (1) silicon wafer, (2) dielectric membrane of four alternating silicon oxide and silicon nitride layers $\text{SiO}_2(0.6 \mu\text{m})/\text{Si}_3\text{N}_4(0.13 \mu\text{m})/\text{SiO}_2(0.3 \mu\text{m})/\text{Si}_3\text{N}_4(0.13 \mu\text{m})$, (3) platinum thermoresistors, (4) platinum heating resistor placed at distance d from the thermoresistors (the color shows the change in temperature (thermal) field distribution under the action of the gas flow).

result in slight membrane stretching, which is necessary for increasing the signal-to-noise ratio in thermoresistive converters by eliminating oscillations typical for some nonstretched membranes.

Another promising direction for the application of thin membranes from a set of $\text{SiO}_2/\text{Si}_3\text{N}_4$ layers in the near future is connected with units of open-vacuum X-ray sources with shot-through membrane targets. In such X-ray sources, the electron beam, passing the membrane, generates X rays with the required wavelength in the film from the given metal with a large atomic number deposited on the membrane. In this case, variants of forming membranes with plane, concave, and convex surfaces [4] should exist for various applications of X-ray sources.

Naturally, silicon oxide SiO_2 and nitride Si_3N_4 films are used in silicon planar technology as dielectric membrane layers. Silicon oxynitride SiO_xN_y films are hardly used for this purpose due to the time and temperature instability of their composition and properties. In order to form a membrane on the back surface of the silicon wafer, most often of KDB-12(100) or KEF-4,5(100) grade oxidized from both sides, photolithography on silicon oxide is applied. Then, liquid chemical or plasma chemical etching of silicon through the whole wafer thickness up to the SiO_2 film on the front surface is then performed through open regions in silicon oxide [5].

The following processes are applied for forming SiO_2 and Si_3N_4 films: high temperature (900–1100°C) thermal oxidation and nitridation, chemical deposition from the gas phase, and both high temperature (500–800°C) without plasma enhancement (chemical vapor deposition (CVD)) and low temperature (200–400°C) with plasma enhancement (plasma enhanced CVD (PECVD)) [6].

The physical deposition of SiO_2 and Si_3N_4 films from the gas phase (physical vapor deposition (PVD)), such as deposition using the reactive magnetron sputtering of silicon targets or the high-frequency sputtering of quartz and silicon nitride targets, are not used for the formation of membrane layers because of the high imperfection of deposited films [7].

The main functional characteristics of membranes for X-ray sources are their high mechanical strength and high transparency to electron beams, and membranes for thermoresistive heat converters, along with high mechanical strength, should possess low heat capacity and heat conduction for good sensor thermal insulation. Moreover, it should be possible to change the shape of the membrane surface by the appropriate choice of mechanical stress in membrane layers.

Obviously, to improve these characteristics it is necessary to reduce the thickness of the standard membrane and, in order to maintain the mechanical strength, it is necessary to use nanostructuring, i.e., form new membranes as sets of silicon dioxide/silicon

nitride ($\text{SiO}_2/\text{Si}_3\text{N}_4$) films with nanometer thickness [8]. The reduction in the thickness of separate layers and the growth in their number in nanostructured membranes would also allow one to monitor more precisely the shape of the membrane surface as required for different applications.

The objective of this study is to develop processes for the formation of nanostructured membranes for MEMS devices and investigate their structure, composition, and parameters.

EXPERIMENT

Thermally oxidized silicon KDB-12(100) wafers with a silicon oxide thickness of 300 nm (0.3 μm) and a diameter of 150 mm were used as blanks for nanostructured membranes. Since silicon wafers with two-sided polish are quite expensive, some blanks were formed from new silicon wafers by their thermal oxidation. The second part of the blanks was formed via the recovery of oxidized wafers by the layer of high temperature silicon nitride with a thickness of 130 nm (0.13 μm) deposited on the oxide surface by removing the Si_3N_4 layer via plasma chemical etching).

Less expensive recovered wafers were used in the development of modes of formation of nanostructured-membrane blanks and the accompanying studies. Blanks of nanostructured membranes from expensive new wafers were used for the production of test samples of gas-flow sensors (Fig. 1).

Sets of alternating Si_3N_4 and SiO_2 films with nanometer thicknesses deposited on thermal silicon oxide were produced at the STS LPX PECVD installation for plasma-enhanced chemical deposition from the gas phase manufactured by SPTS Technologies (Great Britain); a schematic diagram of the working chamber is shown in Fig. 2.

The working chamber represents a diode-type reactor with two plane parallel electrodes. The lower electrode–substrate holder is loaded with the processed silicon wafer (*I*) through the lock. The reactor is pumped out through the exhaust line with the throttling shutter (*5*) by the dry chemically resistant pump to a residual pressure of 3 Pa. Electrodes and walls of the working chamber were heated using three heaters to the following temperatures: lower electrode–substrate holder by heater (*3*) to $T_d = 300^\circ\text{C}$, upper electrode to $T_u = 250^\circ\text{C}$, and chamber walls to $T_w = 75^\circ\text{C}$.

The working gas could be supplied to the working chamber via six gas lines through the gas inlet in the upper electrode and distributed in space via the gas flow collector (*7*). The working pressure for plasma-enhanced chemical deposition from the gas phase was in the range of (30–300) Pa. High frequency (HF) voltage from the RF generator (*6*) with a frequency of 13.56 MHz was supplied to the lower electrode, and an RF discharge was ignited in the working chamber; the decomposition and activation of molecules of the

working gases took place in the plasma of this discharge. Plasma enhancement of the working gases substantially reduces the substrate-holder temperature during chemical deposition in the gas phase when compared to thermal deposition [6].

Voltage from the low frequency (LF) generator (4) with a frequency of 380 kHz could be supplied to the lower electrode–substrate holder. If the voltage from the LF generator was supplied to the lower electrode, its negative displacement with respect to the discharge plasma increased and the energy and intensity of ion bombardment of the dielectric film deposited on the wafer increased. Ion bombardment has almost no influence on the quality of the silicon dioxide films, but it noticeably improves the quality of the silicon nitride layers. Therefore, the voltage from the LF generator was supplied to the lower electrode for Si_3N_4 deposition only.

Tables 1 and 2 give the modes (operational parameters) of the processes of plasma-enhanced chemical deposition from the gas phase of silicon nitride (Si_3N_4) and silicon dioxide (oxide) (SiO_2) films applied in this study at the STS LPX PECVD installation for the production of multilayered nanostructured membranes from sets of $\text{Si}_3\text{N}_4/\text{SiO}_2$ layers deposited on the film of thermal silicon dioxide with a thickness of 0.3 μm .

To determine the deposition time for the sets of $\text{Si}_3\text{N}_4/\text{SiO}_2$ layers with different nanometer thicknesses, single processes with the parameters given in Tables 1 and 2 were applied for test silicon wafers with different deposition times. The thickness of the Si_3N_4 and SiO_2 layers obtained on the test wafers was measured using an Auto SE scanning spectral ellipsometer manufactured by HORIBA Scientific (Japan). The results of these experiments were used to choose the times of the alternating deposition of $\text{Si}_3\text{N}_4/\text{SiO}_2$ layers, according to Tables 1 and 2, in order to form membranes with a Si_3N_4 and SiO_2 film thickness in the range of 100 nm, 50 nm, and 25 nm. The results are given in Table 3.

It should be noted that, according to Tables 1–3, switching of the mode from Si_3N_4 to SiO_2 layer deposition in the formation of multilayered nanostructured

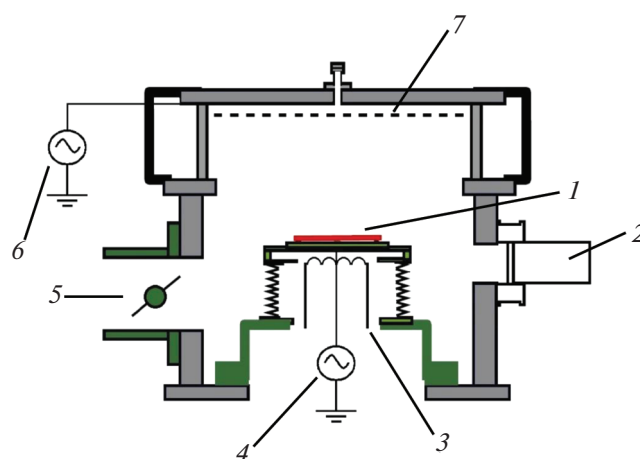


Fig. 2. (Color online) Schematic diagram of the working chamber of the installation for plasma-enhanced chemical deposition from the gas phase of silicon oxide and silicon nitride films STS LPX PECVD manufactured by SPTS Technologies (Great Britain): (1) processed wafer situated on the electrode–substrate holder heated by heater 3—voltage from low frequency (LF) generator 4 with a frequency of 380 kHz can be supplied to this electrode; (2) emission spectrometer for recording plasma parameters in film-deposition processes; (5) pump-out line with the throttle valve; (6) high-frequency (HF) generator with a frequency of 13.56 MHz supplying the voltage to the upper electrode through which working gases are input into the working chamber (reactor); and (7) distributed collector of the gas flow.

membranes from sets of $\text{Si}_3\text{N}_4/\text{SiO}_2$ layers on the working wafers took 60 s by stopping the supply of the applied working gases, the reactor pump-through, and the supply of other working gases.

The STS LPX PECVD installation is capable of providing the deposition of any sets of $\text{Si}_3\text{N}_4/\text{SiO}_2$ layers in the automatic mode; for this purpose, it is necessary to code the deposition modes (recipes) in its control computer and set these modes as the working ones. In order to try out the modes of formation of multilayered nanostructured membranes from sets of $\text{Si}_3\text{N}_4/\text{SiO}_2$ layers, the Si_3N_4 and SiO_2 layer deposition modes were switched manually by corresponding commands.

Table 1. Operational parameters of plasma-enhanced chemical deposition from the gas phase of silicon nitride (Si_3N_4) films at the STS LPX PECVD installation

Silane flow rate $Q(\text{SiH}_4)$, cm^3/min	Ammonia flow rate $Q(\text{NH}_3)$, cm^3/min	Nitrous oxide flow rate $Q(\text{N}_2\text{O})$, cm^3/min	Working pressure p , Pa	Generator power W , W	Generator type
25	55	1960	120	100	HF
25	55	1960		30	LF
		1960		100	HF

The duration of the last stage of the process consisting of ion bombardment of the deposited Si_3N_4 film is 2 min (120 s).

the upper light layer is titanium film applied on the wafer surface for the electric charge drain.

A photo of the nanostructured membrane **m2** blank is shown in Fig. 3b. It contains fourteen alternating $\text{SiO}_2/\text{Si}_3\text{N}_4$ layers instead of the set sixteen layers, since the SiO_2 layer between the fifth and the sixth Si_3N_4 layers is missing and the doubled Si_3N_4 layer has a doubled thickness of 88.1 nm, unlike the other Si_3N_4 layers (the layers are enumerated upward). This is connected with the fact that the operator missed one of the switchings from the Si_3N_4 to SiO_2 film deposition mode.

The photo of the nanostructured membrane **m3** (Fig. 3c) shows all 28 sets of alternating $\text{SiO}_2/\text{Si}_3\text{N}_4$ layers. It can be seen, however, that the thickness of the lowermost Si_3N_4 layer is larger than 100 nm, which testifies that the layer of high temperature silicon nitride was not etched off the membrane blank in the course of wafer recovery and additional deposition of the Si_3N_4 layer in the high-temperature plasma enhanced process.

To determine the elemental composition and stoichiometry of SiO_2 and Si_3N_4 layers, we used the SIMS and AES methods. These methods were also used for a more precise determination of the thickness of the layers, since the “smearing” of the cross-section image obtained with secondary electrons for the sets of $\text{SiO}_2/\text{Si}_3\text{N}_4$ layers using SEM prevented a precise measurement of the thickness of separate silicon oxide and nitride films in the blanks of the nanostructured membranes.

The element-distribution profile into the sets of $\text{SiO}_2/\text{Si}_3\text{N}_4$ layers on the membranes was obtained using the new-generation TOF.SIMS 5 SIMS system manufactured by IONTOF (Germany).

The SIMS method is based on the physical sputtering of surface atomic layers of a specimen by a beam of high-energy ions called “primary ions.” Hitting the specimen’s surface, the primary ion causes a cascade of collisions resulting in sputtering of the specimen material both in the form of neutral and charged particles, “secondary ions.” An analysis of secondary ions provides information on the elemental and isotopic composition of the material in the studied area. In the mass spectrometric analysis of the sputtered material, secondary ions form the secondary ion beam, are accelerated, are sorted with respect to the mass-to-charge ratio, and the signal intensity is detected.

The TOF.SIMS 5 system applies a new principle of two ion beams, the synchronous alternation of pulsed analyzing and sputtering beams. Moreover, the TOF.SIMS 5 system presents fundamentally new capabilities for an analysis of dielectric structures, as well as poorly conducting thin film structures on dielectric substrates, which often presents an unsolvable problem in dynamic SIMS systems.

For this purpose, the TOF.SIMS 5 system contains an additional low-energy electron gun operating in the pulsed mode. The electron beam completely neutralizes the charge caused by the analyzing low-current ion beam. To compensate the charge caused by sputtering ion beams with a much higher current (hundreds of nA), additional time delays in the “sputtering—analysis” sequence are introduced in a wide range from units of microseconds to several seconds [9].

An analysis of the specimens of nanostructured membrane blanks in the TOF.SIMS 5 system was performed under the following conditions:

(i) etching of a crater in membranes by cesium Cs^+ ions with an energy of 1 keV on a $300 \times 300 \mu\text{m}$ pattern;

(ii) analyzing beam of bismuth (Bi^+) ions with a current of 1.5 pA had an energy of 30 keV and a pattern of $100 \times 100 \mu\text{m}$;

(iii) for measuring the depth of the ion etched crater, an Alpha-Step D-120 contact profilometer manufactured by KLA-Tencor Instruments (United States) was applied.

The SIMS element-distribution profiles obtained in the TOF.SIMS 5 system in the specimens of nanostructured membrane **m1**, **m2**, and **m3** blanks are shown in Fig. 4.

It can be seen from Fig. 4a that the blanks of membrane **m1** have eight preset alternating $\text{SiO}_2/\text{Si}_3\text{N}_4$ layers with the following thicknesses: $\text{SiO}_2(300 \text{ nm})/\text{Si}_3\text{N}_4(100 \text{ nm})/\text{SiO}_2(80 \text{ nm})/\text{Si}_3\text{N}_4(100 \text{ nm})/\text{SiO}_2(80 \text{ nm})/\text{Si}_3\text{N}_4(100 \text{ nm})/\text{SiO}_2(80 \text{ nm})/\text{Si}_3\text{N}_4(100 \text{ nm})$. Therefore, unlike the case of depositing a SiO_2 film with a thickness of 100 nm calculated with the help of a test wafer in a single process, the thickness of a SiO_2 layer formed in one of the alternating processes of plasma-enhanced chemical $\text{Si}_3\text{N}_4/\text{SiO}_2$ deposition from the gas phase is reduced by 20 nm (or 20%) for the same deposition time. The thickness of the Si_3N_4 film of 100 nm corresponds to the thickness calculated by the deposition time of the silicon nitride layer onto the test wafer in a single process.

Figure 4b shows that the specimen of membrane **m2** blank has fourteen alternating $\text{SiO}_2/\text{Si}_3\text{N}_4$ layers instead of sixteen layers. The layers have the following thicknesses: $\text{SiO}_2(300 \text{ nm})/\text{Si}_3\text{N}_4(47 \text{ nm})/\text{SiO}_2(34 \text{ nm})/\text{Si}_3\text{N}_4(47 \text{ nm})/\text{SiO}_2(34 \text{ nm})/\text{Si}_3\text{N}_4(47 \text{ nm})/\text{SiO}_2(34 \text{ nm})/\text{Si}_3\text{N}_4(47 \text{ nm})/\text{SiO}_2(34 \text{ nm})/\text{Si}_3\text{N}_4(94 \text{ nm})/\text{SiO}_2(34 \text{ nm})/\text{Si}_3\text{N}_4(47 \text{ nm})/\text{SiO}_2(34 \text{ nm})/\text{Si}_3\text{N}_4(47 \text{ nm})$. It can be seen that the SiO_2 layer between the 5th and 6th Si_3N_4 layers is missing, and the doubled Si_3N_4 layer has a doubled thickness of 94 nm, unlike the other layers. According to the calculation of the deposition time using the test wafer in single processes, Si_3N_4 and SiO_2 films should have a thickness of 50 nm. While the thickness of the silicon nitride layer obtained in the alternating processes of plasma-enhanced chemical deposition from

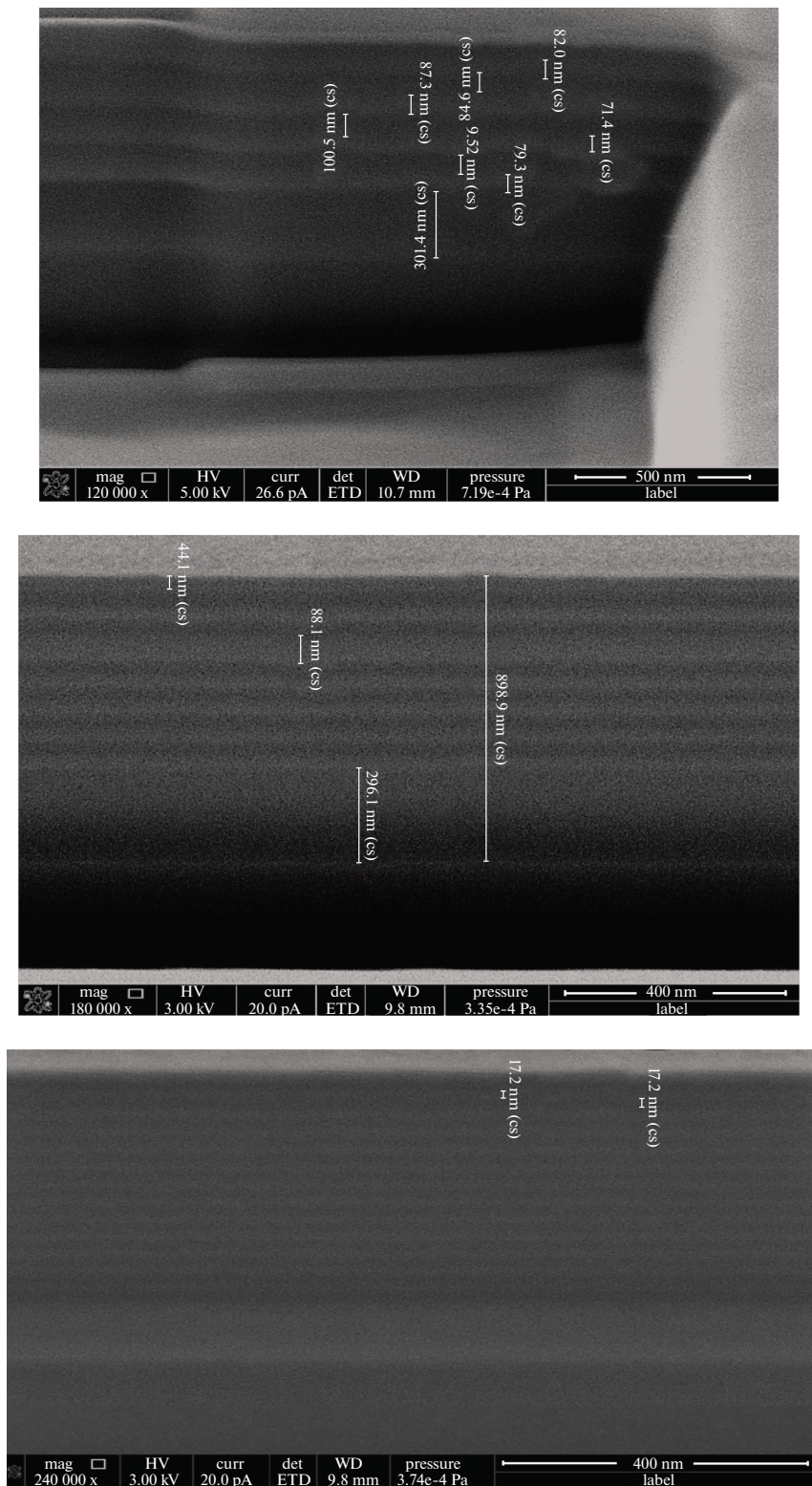


Fig. 3. (Color online) Photos of secondary electron images of transverse cuts for specimens of nanostructured membrane blanks: (a) specimen of membrane **m1** blank consisting of eight preset alternating SiO₂/Si₃N₄ layers (Si₃N₄ layers have a lighter background than SiO₂ layers, and the upper light layer is a titanium film applied on the wafer surface for charge drain); (b) specimen of membrane **m2** blank consisting of 14 alternating SiO₂/Si₃N₄ layers instead of the preset 16 layers: the SiO₂ layer between the fifth and sixth Si₃N₄ layers is missing, and the doubled Si₃N₄ layer has a doubled thickness of 88.1 nm, unlike other Si₃N₄ layers (layers are enumerated upward); and (c) specimen of membrane **m3** blank consisting of 28 preset alternating SiO₂/Si₃N₄ layers (it can be seen that the lowermost Si₃N₄ layer has a thickness larger than 100 nm, which indicates that the layer of high temperature silicon nitride was not etched off the membrane blank).

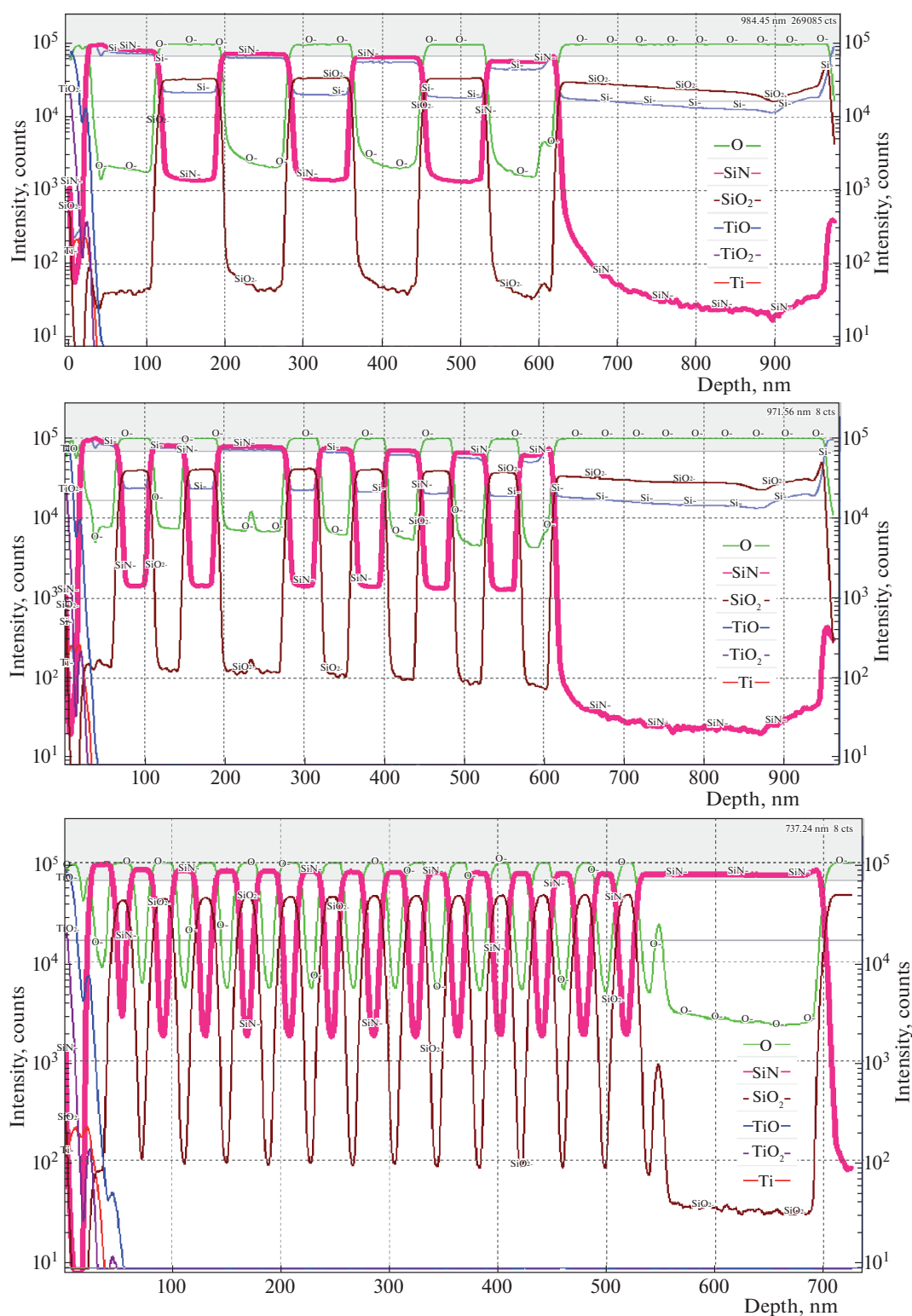


Fig. 4. (Color online) Element distribution over depth obtained by SIMS in specimens of nanostructured membrane blanks: (a) the specimen of the membrane **m1** blank has eight preset alternating SiO₂/Si₃N₄ layers and a layer of titanium and its oxides with a thickness of at least 20 nm on the surface; (b) specimen of the membrane **m2** blank has 14 alternating SiO₂/Si₃N₄ layers instead of the preset 16 layers and a layer of titanium and its oxides with a thickness of at least 20 nm on the surface (the SiO₂ between the fifth and sixth Si₃N₄ layers is missing and the doubled Si₃N₄ layer has a doubled thickness of 94 nm, unlike the other layers); and (c) specimen of the membrane **m3** blank in SIMS analysis was etched to a film of thick thermal oxide followed by a peak of the first thick (160 nm) silicon nitride layer; therefore, the membrane blank has 28 alternating SiO₂/Si₃N₄ layers and a layer of titanium and its oxides with a thickness of at least 20 nm on the surface.

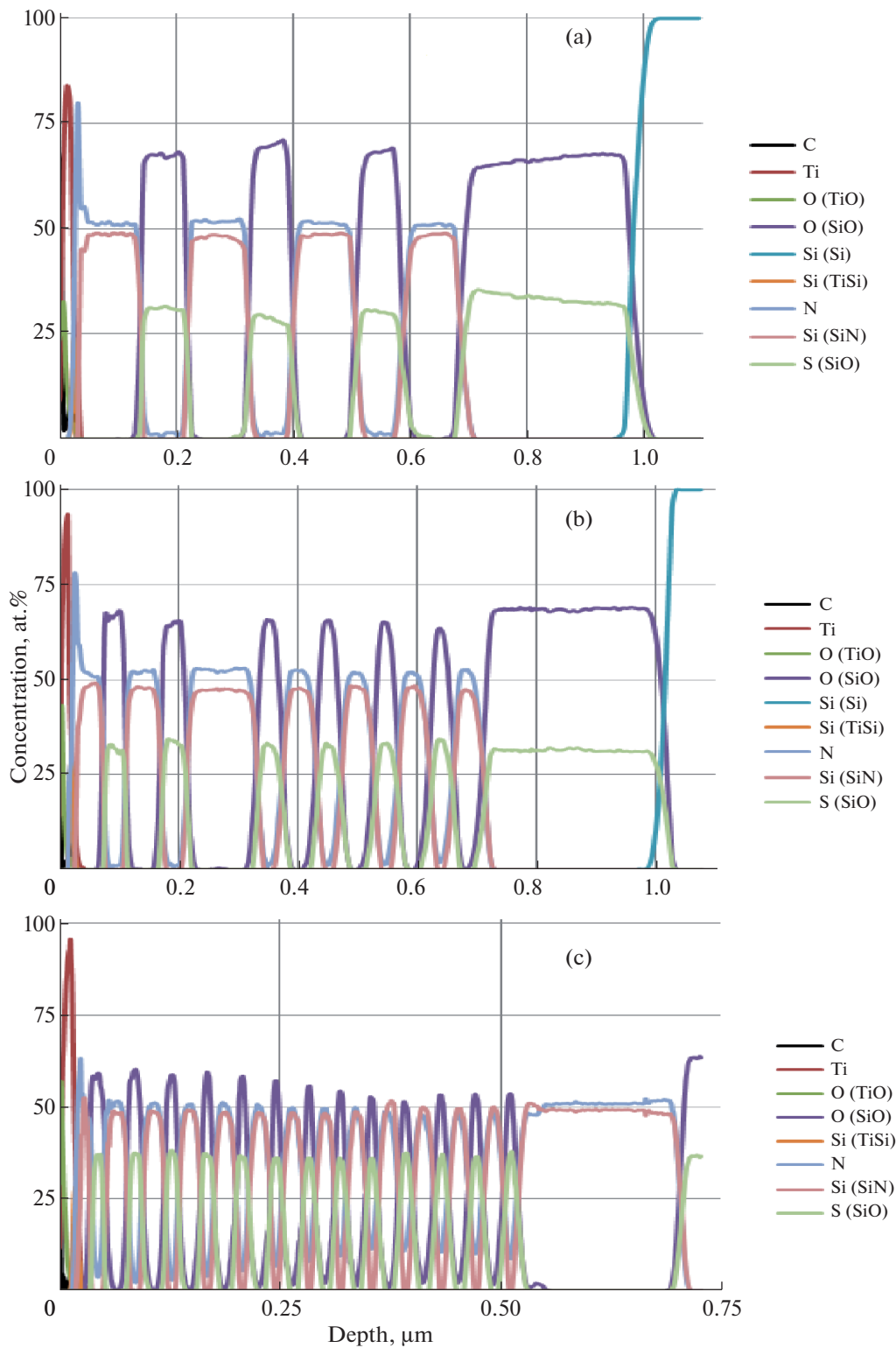


Fig. 5. (Color online) Element distribution over depth obtained by AES in specimens of nanostructured membrane blanks: (a) specimen of the membrane **m1** blank has eight preset alternating SiO₂/Si₃N₄ layers and a layer of titanium and its oxides on the surface; (b) specimen of the membrane **m2** blank has 14 alternating SiO₂/Si₃N₄ layers instead of the preset 16 layers and a layer of titanium and its oxides on the surface (the SiO₂ between the fifth and sixth Si₃N₄ layers is missing and the doubled Si₃N₄ layer has a doubled thickness of about 100 nm, unlike the other layers); and (c) specimen of membrane **m3** blank in AES analysis was etched to a film of thick thermal oxide followed by a peak of the first thick (160 nm) silicon nitride layer; therefore, the membrane blank has 28 alternating SiO₂/Si₃N₄ layers and a layer of titanium and its oxides on the surface.

Table 4. Calculated average thicknesses of alternating SiO₂/Si₃N₄ layers deposited in plasma-enhanced processes on specimens of nanostructured **m1**, **m2**, and **m3** membrane blanks

Membrane blank specimen	SiO ₂ layer thickness, nm	Si ₃ N ₄ layer thickness, nm	Thickness of the pair of layers SiO ₂ and Si ₃ N ₄ , nm
m1	81.3	100.7	182
m2	40.3	55.2	95.5
m3	15.2	23.8	39

the gas phase is close to this value, the thickness of the silicon dioxide layer is 16 nm smaller (almost 30%).

According to Fig. 4c, the etching of the specimen of nanostructured membrane **m3** blank in the course of SIMS analysis was performed for a film of thick (300 nm) thermal silicon oxide, which is the first in the series of layer peaks in the right upper corner. It can be seen, however, that the first Si₃N₄ layer has a thickness of 160 nm, which testifies that the layer of high-temperature Si₃N₄ was not etched off the membrane blank in the recovery of the silicon wafer and the subsequent deposition of the Si₃N₄ layer in the low-temperature plasma-enhanced process.

Taking into account this condition, the specimen of membrane **m3** blank has all 28 preset alternating SiO₂/Si₃N₄ layers with the following thicknesses: SiO₂(300 nm)/Si₃N₄(160 nm)/SiO₂(15 nm)/Si₃N₄(27 nm).

According to the deposition time for the test wafer in single processes, the Si₃N₄ and SiO₂ films on the specimen of membrane **m3** blank should have a thickness of 25 nm. The thickness of the Si₃N₄ layer obtained in the alternating processes of plasma-enhanced chemical deposition from the gas phase is close to this value, while the thickness of the SiO₂ layer is 10 nm smaller (by 40%).

It should be noted that the precision of determining layer thickness by element distribution profiles obtained using SIMS analysis depends on the ratio of etching rates for silicon nitride and oxide layers by cesium ions; the closer the etching rates are, the more precisely the layer thickness is determined. The etching rates for the SiO₂ and Si₃N₄ films by argon ions with an energy of 1 keV differ by less than 10% [10], while for cesium ions these rates should be determined for particular studied films.

To determine the elemental composition of the set of Si₃N₄/SiO₂ layers produced on specimens of the membrane blanks in the alternating processes of plasma-enhanced chemical deposition from the gas

phase and a more precise measurement of their thickness, the specimens were studied using the AES method on a PHI-670xi AES spectrometer manufactured by Physical Electronics (United States). The profile Auger analysis of the studied specimens was performed under the following conditions:

- (i) accelerating voltage of the primary electron beam 10 kV;
- (ii) primary electron-beam current 20 nA;
- (iii) accelerating voltage of argon (Ar⁺) ion beam 3 kV;
- (iv) ion-beam current 0.6 μA;
- (v) diameter of the averaging region for Auger signal detection 170 μm.

The element concentrations were calculated according to the model of homogeneous distribution using the method of relative inverse-element sensitivity coefficients [11]. The relative element sensitivity coefficients for nitrogen, oxygen, silicon, and titanium were obtained in advance at test specimens of thermal silicon oxide, silicon nitride, and titanium oxide.

To obtain element distribution over the depth of the nanostructured membrane blanks, the average ion sputtering rate for silicon dioxide and nitride was determined. It was calculated using the depth of membrane ion etching crater measured on an Alpha-Step D-120 contact profilometer manufactured by KLA-Tencor (United States) and the time of its formation.

To determine the thickness of the titanium layer, a separate profile Auger analysis of the titanium layer was performed. A thickness of this layer of 13 nm was found from the depth of the ion-etching crater in the titanium layer.

Figure 5 shows the element distribution over the depth of nanostructured membrane **m1**, **m2**, and **m3** blanks. The following conclusions on the topology of the alternating SiO₂/Si₃N₄ layers on the membrane blanks can be made from an analysis of these profile distributions:

- (i) all eight preset SiO₂ and Si₃N₄ layers are present on the specimen of the membrane **m1** blank (Fig. 5a);
- (ii) the SiO₂ layer between the fifth and sixth Si₃N₄ layers is missing and the doubled Si₃N₄ layer has a doubled thickness on the specimen of the membrane **m2** blank (Fig. 5b);
- (iii) one additional (nonpreset) silicon nitride layer with a thickness of ~160 nm is present between the first layer of thermal oxide and the periodic Si₃N₄/SiO₂ layers deposited from the chemical phase

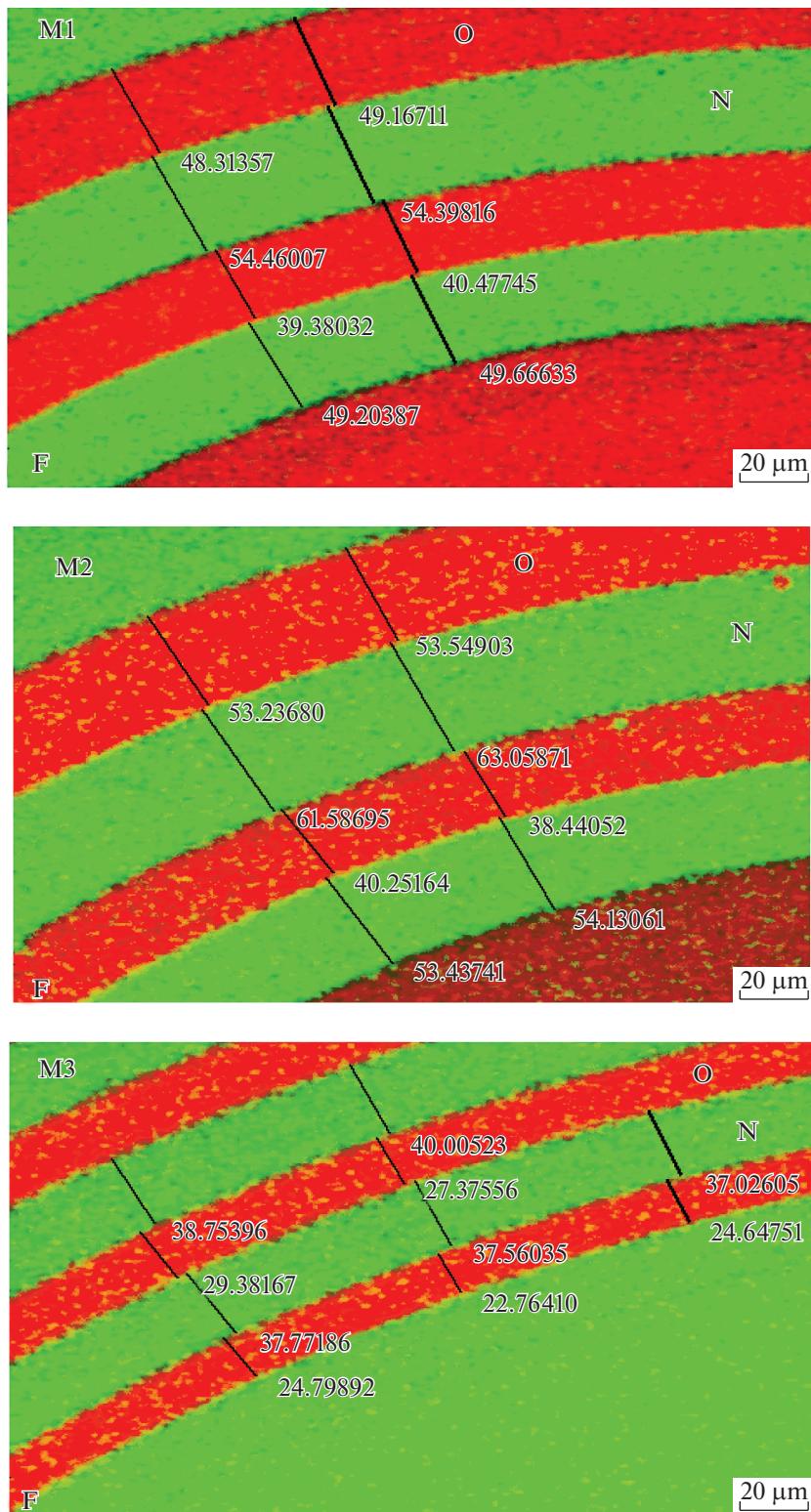


Fig. 6. (Color online) Superposed image obtained using (red) oxygen and (green) nitrogen Auger electrons for ion-etched craters (angle laps) in specimens of nanostructured membrane blanks: (a) specimen of the **m1** membrane blank, (b) specimen of the **m2** membrane blank, and (c) specimen of the **m3** membrane blank.

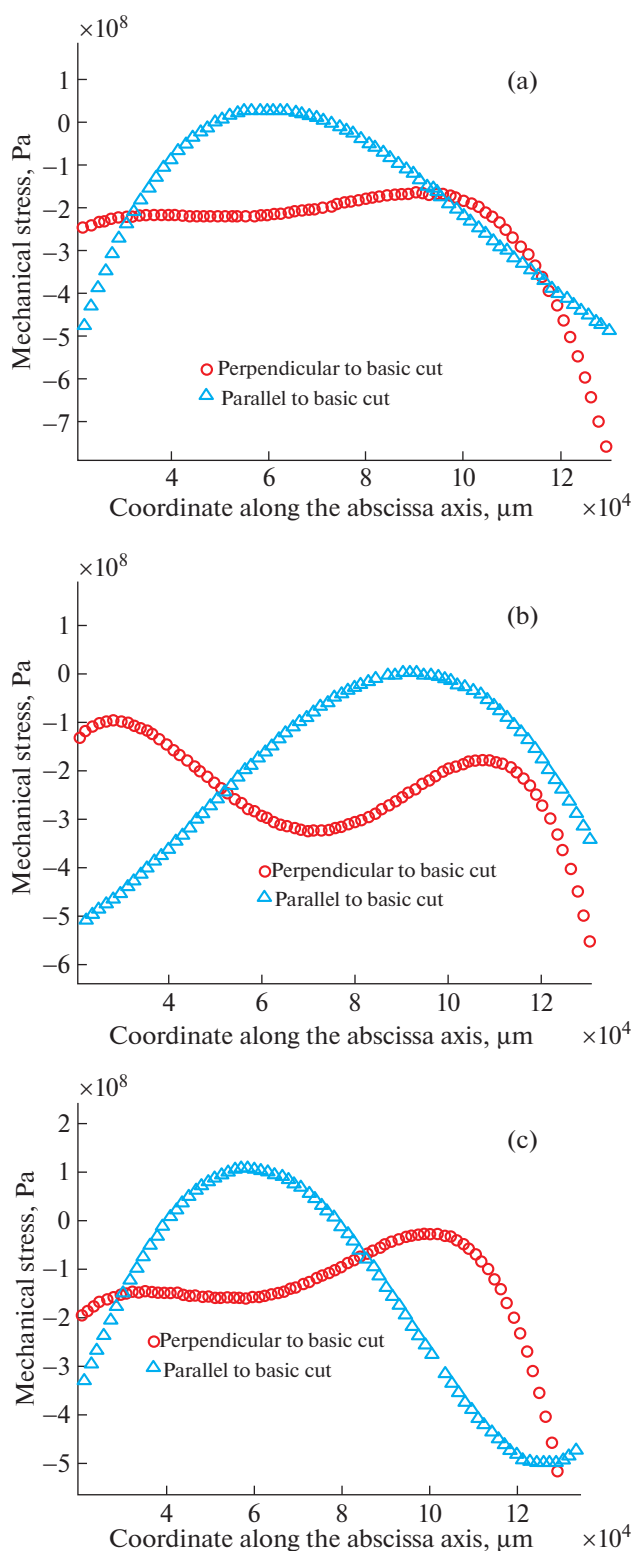


Fig. 7. (Color online) Experimental determination of mechanical stress in wafers with nanostructured membrane blanks: (a) specimen of the **m1** membrane blank, (b) specimen of the **m2** membrane blank, and (c) specimen of the **m3** membrane blank.

in the plasma-enhanced processes on the specimen of the membrane **m3** blank (Fig. 5c).

The periodic $\text{Si}_3\text{N}_4/\text{SiO}_2$ layers deposited on the membrane blanks from the chemical phase in the plasma-enhanced processes with the modes given in Tables 1–3 had the following stoichiometry: silicon oxide corresponded to the formula $\text{SiO}_{2.2}$ and silicon nitride corresponded to formula $\text{Si}_{0.48}\text{N}_{0.52}$. Moreover, all layers of this silicon oxide on all membrane blanks contained nitrogen with a concentration of (1–2 at %), which is connected with the use of nitrous oxide (N_2O) as the oxidizer and nitrogen as the carrier gas.

To more precisely determine the thickness of alternating $\text{SiO}_2/\text{Si}_3\text{N}_4$ layers on the specimens of nanostructured membrane **m1**, **m2**, and **m3** blanks, the studied specimens were processed on an ion etching and polishing Model 1060 SEM Mill installation manufactured by Fischione Instruments (United States) to form an ion-etching crater (angle lap) at an angle of less than 10° to the surface. The image obtained using oxygen and nitrogen Auger electrons in thus prepared specimens of nanostructured membrane **m1**, **m2**, and **m3** blanks are shown in Fig. 6.

The craters (angle laps) were used to measure the relative thickness of dielectric layers on the specimens of nanostructured membrane blanks. The average rate of the ion etching of craters was used to calculate the thickness of pairs of silicon oxide and nitride layers on the specimens of membrane blanks. Thus, the average thicknesses of alternating $\text{SiO}_2/\text{Si}_3\text{N}_4$ layers deposited in plasma-enhanced processes on the specimens of nanostructured membrane **m1**, **m2**, and **m3** blanks given in Table 4 were obtained.

It can be seen from a comparison of the data given in Tables 3 and 4 that the times of silicon nitride layer deposition in the plasma-enhanced processes required for obtaining a layer thickness of 100 nm, 50 nm, and 25 nm were chosen correctly. At the same time, the times of silicon oxide layer deposition in the plasma-enhanced processes required for obtaining a layer thickness of 100, 50, and 25 nm in the processes given in Table 2 should be increased, when compared to the data in Table 3, to 140, 66, and 44 s, respectively.

The SIMS and AES results were used to calibrate the SmartLab multifunctional X-ray diffractometer manufactured by Rigaku (Japan), which, when verified, can be used to monitor the similarity of qualitative and quantitative parameters of nanostructured membrane blanks on 150 mm silicon wafers without their destruction or the deposition of auxiliary layers, for example, a titanium layer for electric charge drain.

A SmartLab X-ray diffractometer was used to select wafers without missing or nonpreset SiO_2 and Si_3N_4 layers among nanostructured membrane **m1**, **m2**, and **m3** blanks. The mechanical stress was determined for these wafers before using them in the process of manufacturing platinum thermoresistive sensors.

The mechanical stress was determined according to the method described in [11]. The method is based on the Stoney technique [12], in which the current mechanical stress is calculated by the measured plate

bending from the curvature radius of a local plate surface area.

The wafer regions with nanostructured membrane blanks were in the range of (20–130 mm). Figure 7 shows the experimental dependence of mechanical stress in the direction perpendicular and parallel to the basic cuts of wafers with nanostructured membrane **m1**, **m2**, and **m3** blanks. The calculated average mechanical stress in the working region of the wafers with nanostructured membrane blanks are as follows: for the wafer with membrane **m1** blank, 328 MPa; for the wafer with membrane **m2** blank, 286 MPa; and, for the wafer with membrane **m3** blank, 234 MPa.

Therefore, with the decreasing thickness of alternating $\text{Si}_3\text{N}_4/\text{SiO}_2$ layers and increasing number of layers in the membrane structure, the absolute value of mechanical stress of wafers with membrane blanks decreases. The mechanical strength of the membranes increases due to growing interfaces between layers, since multiple interfaces complicate the growth of global mechanical defects in membranes.

CONCLUSIONS

A technology of forming blanks of nanostructured membranes for MEMS devices based on alternating $\text{Si}_3\text{N}_4/\text{SiO}_2$ layers with a thickness of 100, 50, and 25 nm, chemically deposited from the gas phase in low-temperature plasma-enhanced processes, was developed.

Three designs of nanostructured membrane blanks consisting of the layer of thermal silicon oxide with a thickness of 300 nm and 7 alternating Si_3N_4 (100 nm)/ SiO_2 (100 nm) layers, 15 alternating Si_3N_4 (50 nm)/ SiO_2 (50 nm) layers, and 27 alternating Si_3N_4 (25 nm)/ SiO_2 (25 nm) layers were produced.

An integrated investigation of the structure, composition, and parameters of the three designs of nanostructured membrane blanks was performed using the following microanalysis methods: spectral ellipsometry, scanning electron microscopy, secondary ion mass spectrometry, Auger electron spectroscopy, probe profilometry, and X-ray diffractometry.

The studies revealed the following defects in the nanostructured membrane blanks:

(i) the absence of one SiO_2 layer on membrane **m2** blank caused by the error of the operator, who missed one switching from the Si_3N_4 to the SiO_2 film-deposition mode;

(ii) the presence of an additional Si_3N_4 layer on the membrane **m2** blank, testifying that the layer of high-temperature silicon nitride was not etched off the membrane blank in the course of wafer recovery and an additional deposition of the Si_3N_4 layer in the low-temperature plasma enhanced process;

(iii) a different thickness of SiO_2 films deposited on membrane blanks alternating with Si_3N_4 layers and SiO_2 films deposited in single processes on test silicon wafers.

These studies contributed to the development of technological modes of formation of nanostructured membrane blanks based on periodically alternating $\text{Si}_3\text{N}_4/\text{SiO}_2$ layers with a layer thickness of 100, 50, and 25 nm.

It was shown that all periodically alternating $\text{Si}_3\text{N}_4/\text{SiO}_2$ layers in blanks of all nanostructured membranes had the following stoichiometry: silicon oxide corresponded to the formula $\text{SiO}_{2.2}$, and silicon nitride corresponded to the formula $\text{Si}_{0.48}\text{N}_{0.52}$. Moreover, nitrogen with a concentration of (1–2 at %) was present in all silicon oxide layers.

The mechanical stress on the wafers with nanostructured membrane blanks was measured; the measurements showed that the absolute value of mechanical stress in the wafers decreases with a decreasing thickness and increasing number of periodic $\text{Si}_3\text{N}_4/\text{SiO}_2$ layers.

ACKNOWLEDGMENTS

This work was supported by the Ministry of Education and Science of the Russian Federation, agreement no. 14.578.21.0188, unique identifier RFMEFI57816X0188, using equipment of the Microsystem Equipment and Electron Component Base Collective Use Center.

REFERENCES

1. C. Zorman, *Material Aspects of Micro- and Nanoelectromechanical Systems*, Springer Handbook of Nanotechnology (Springer, Berlin, 2007).
2. D. Urmanov, *Elektron.*: Nauka, Tekhnol., Biznes, No. 1, 192 (2013).
3. N. Dyuzhev, D. Novikov, and V. Ryabov, *Solid State Phenom.* **245**, 247 (2016).
4. D. Bernard, *Tekhnol. Elektron. Prom-sti*, No. 4, 48 (2010).
5. G. S. May and C. J. Spanos, *Fundamentals of Semiconductor Manufacturing and Process Control* (Wiley, New Jersey, 2006).
6. *Handbook of Semiconductor Manufacturing Technology*, Ed. by Y. Nishi and R. Doering, 2nd ed. (Marcell Dekker, New York, 2008).
7. *Handbook of Semiconductor Interconnection Technology*, Ed. by G. C. Schwartz and K. V. Srikrishnan, 2nd ed. (CRC, Taylor Francis Group, New York, 2006).
8. V. Yu. Kireev, *Introduction to Microelectronics Technologies and Nanotechnologies* (TsNIIKhM, Moscow, 2008) [in Russian].
9. TOF.SIMS 5 brochure. www.iontof.com.
10. N. V. Pleshivtsev and A. I. Bazhin, *Physics of Ion Beams Effect on the Materials* (Vuzovskaya Lniga, Moscow, 1998) [in Russian].
11. *Practical Surface Analysis by Auger and X-ray Photoelectron Spectroscopy*, Ed. by D. Briggs and M. Seah (Wiley, New York, 1983).
12. N. A. Dyuzhev, A. A. Dedkova, E. E. Gusev, and A. V. Novak, *Izv. Vyssh. Uchebn. Zaved., Elektron.*, No. 4, 367 (2016).
13. G. G. Stoney, *Proc. R. Soc. London A* **82**, 172 (1909).

SPELL: OK

Translated by E. Baldina